LHC EVENT GENERATION WITH GENERAL-PURPOSE MONTE CARLO TOOLS*

Andrzej Siódmok

Consortium for Fundamental Physics, School of Physics and Astronomy
The University of Manchester, Manchester, UK

(Received June 17, 2013)

We briefly describe the building blocks of general-purpose Monte Carlo event generators for the full simulation of the proton–proton collisions at the LHC. Then, we present a comparison of three main Monte Carlo event generators, HERWIG, PYTHIA and SHERPA to a range of the LHC data.

DOI:10.5506/APhysPolB.44.1587
PACS numbers: 12.38.–t, 13.85.Hd, 21.60.Ka

1. Introduction

Monte Carlo event generators (MCEG) are central-to-high energy particle physics. They are used in the analysis of almost all experimental data to simulate the event features of signal processes and their backgrounds. Unfortunately, *"... it often happens that the physics simulations provided by the MC generators carry the authority of data itself. They look like data and feel like data, and if one is not careful they are accepted as if they were data"* (extracted from a talk by Bjorken [1]). Therefore, it is important to understand the assumptions and approximations involved in these simulations to be able to answer the following type of questions. Is the effect I am seeing due to different models, or approximations, or is it a bug? Am I measuring a fundamental quantity or merely a parameter in the simulation code? In this contribution, we briefly describe the building blocks of a Monte Carlo event generation[1] and focus on comparison of the three main MCEG HERWIG++ [3–5], PYTHIA [6, 7] and SHERPA [8, 9] against the recent Large Hadron Collider (LHC) data.

* Presented at the Cracow Epiphany Conference on the Physics After the First Phase of the LHC, Kraków, Poland, January 7–9, 2013.

[1] For a detailed description of MCEG with much more information on the physics background, we refer the Reader to the MCnet review paper on Monte Carlo event generators [2].

2. Event generation

The structure of a proton–proton collision at the LHC as built up by MCEG can be described by a few main building blocks:

1. Hard process;
2. Parton shower;
3. Hadronization;
4. Multiple Interactions;
5. Decays of unstable hadrons.

In Fig. 1, we show a drawing of the event generation (excluding multiple interactions). The generation starts with a hard signal process, for example, in the figure this is a pair of leptons production (black/red). Then, the parton showers (PS) evolution (marked with the dark and light grey/green gluon curly lines) starts from the hard process and works downwards to lower and lower momentum scales to a point ~ 1 GeV, where perturbation theory breaks down. At this scale, the partonic degrees of freedom are converted into hadrons (light grey/yellow circles) via a hadronization model. In the case of Fig. 1, the cluster hadronization model (white blobs) is presented. The last step of event generation is based on the fact that many of these hadrons (light grey/yellow blobs) are not stable particles and, therefore, they decay. In addition to this sequence of steps, all initiated by the hard

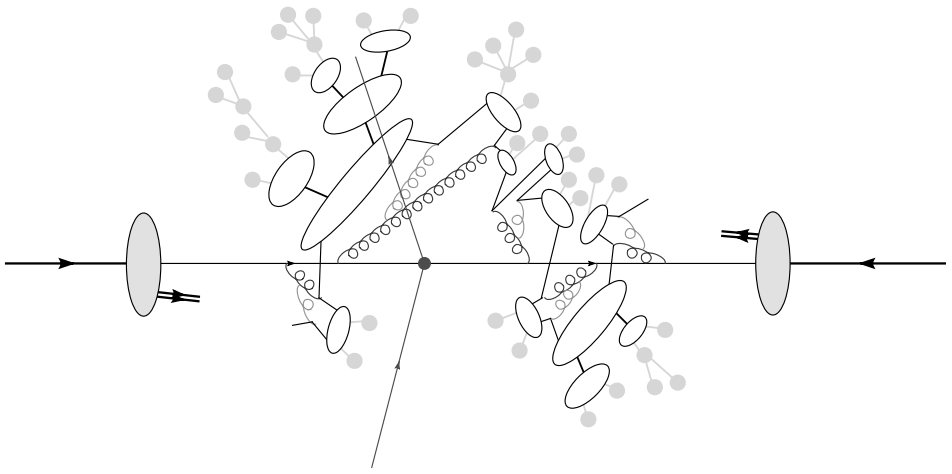

Fig. 1. (Colour online) Drawing of the simulation of a pp collision shown in [10]. The multiple interactions are not included in this figure.

subprocess, there may be additional semi-hard processes, called multiple partonic interactions. These are mostly fairly soft QCD interactions that also undergo all steps described above for the hard process and produce additional particles in all the available phase space. This brief overview of a process from hard collision to stable hadrons is effectively used by all current MCEG, although some details and physics emphasis differ:

— PYTHIA[2] is a successor of the JETSET [11] (begun 1978). Traditionally, PYTHIA has put strong emphasis on soft physics, such as hadronization (it grown out of the well developed Lund string model), minimum-bias physics and the soft underlying event.

— HERWIG — **H**adron **E**mission **R**eactions **W**ith **I**nterfering **G**luons is a successor to the ERWIG (begun in 1984). Traditionally, HERWIG has put its emphasis on the perturbative description of an event and has originated in the coherence studies leading to angular ordered parton shower. Hadronization uses the cluster model.

— SHERPA — **S**imulation of **H**igh-**E**nergy **R**eactions of **PA**rticles (begun in 2000). Originated in merging of leading-order matrix elements for multijet production with parton showers (CKKW [12]). Provided by two independent matrix element generators. Hadronization model is similar to the cluster model used in HERWIG.

3. Hard matrix element

The starting point of the simulation, the generation of tree level processes is fairly straightforward. SHERPA is provided by two independent matrix element generators COMIX [13] and AMEGIC++ [14] for large final state multiplicities in various models, and interfaced to an automated Feynman rule generator. HERWIG++ and PYTHIA both have a large set of hand-coded matrix elements for the most common subprocesses for hadron, lepton and DIS collisions. Modelling physics beyond the Standard Model is also available in both programs [15–17]. For example, HERWIG++ has automatic generation of hard processes and decays with full spin correlations for many BSM models, which has recently been used to confront a large class of gauge mediation models with the LHC data on jets plus missing energy [18]. On top of this, the latter two generators allow parton-level events with any number of legs to be read from external sources like MadEvent [19] using Les Houches Event File (LHEF) [20].

[2] The explanation of the "Pythia" label is provided in Appendix to the PYTHIA's manual [6].

Sometimes MCEG are called Leading Order Monte Carlo Event generators. This name is not always correct since all modern MCEG incorporate, for several processes, the full NLO corrections merged to the parton shower. This very important topic will be mentioned in the next section and since is covered by van Hameren [21] in a separate contribution to this conference will not be discussed here in more details.

4. Parton shower

The basic idea of the parton shower is to set up in a probabilistic way a simulation of the cascade of partons that is produced by the colour partons that come out of hard process. In principle, the showers represent higher-order corrections to the hard subprocess. However, it is not feasible to calculate these corrections exactly. Instead, an approximate scheme is used, in which the dominant contributions are included in each order. These dominant contributions are associated with collinear parton splitting or soft (low-energy) gluon emission. Over the last decade, parton shower modelling has been a very active field. This led to a number of refinements in shower algorithms and, moreover, the construction of new parton showers.

The successor of fortran HERWIG [22, 23], HERWIG++, was based on the reformulation of angular ordered parton showers for massive particles [24]. There was also an attempt to extend the PS evolution to the non-perturbative region [25]. PYTHIA uses now transverse momentum ordered parton showers that are interleaved with multiple partonic interactions [26, 27]. SHERPA's default parton-shower algorithm [28] is based on the Catani–Seymour dipole factorization formalism [29]. SHERPA has also implemented a shower [30] that is based on dipoles similar to the ones used in the ARIADNE program [31]. In HERWIG++, there is also an option to use a shower based on subtraction terms [32]. The VINCIA approach [33–35], which is an add-on module for PYTHIA, employs antenna subtraction terms to formulate the parton showers.

Instead of going into the details of different PS approaches implemented in MCEG, we show their comparison to several observables measured at the LHC that are sensitive to the cascade radiation. In Fig. 2, we see the transverse momentum spectrum of $Z/\gamma*$ in a Drell–Yan process measured by the ATLAS Collaboration. During the Initial State Radiation (ISR PS evolution), the recoil from the emitted partons (mainly gluons) builds up a transverse momentum for the boson[3]. As we can see, all MCEG describe this observable well. The other observable that is sensitive to collinearly emitted particles, this time in the final state, is the internal jet shape (energy flow)

[3] Sweeping across the distribution, one has regions dominated by hard perturbative emission, multiple soft and/or collinear, but still perturbative, emission, and truly non-perturbative confinement effects.

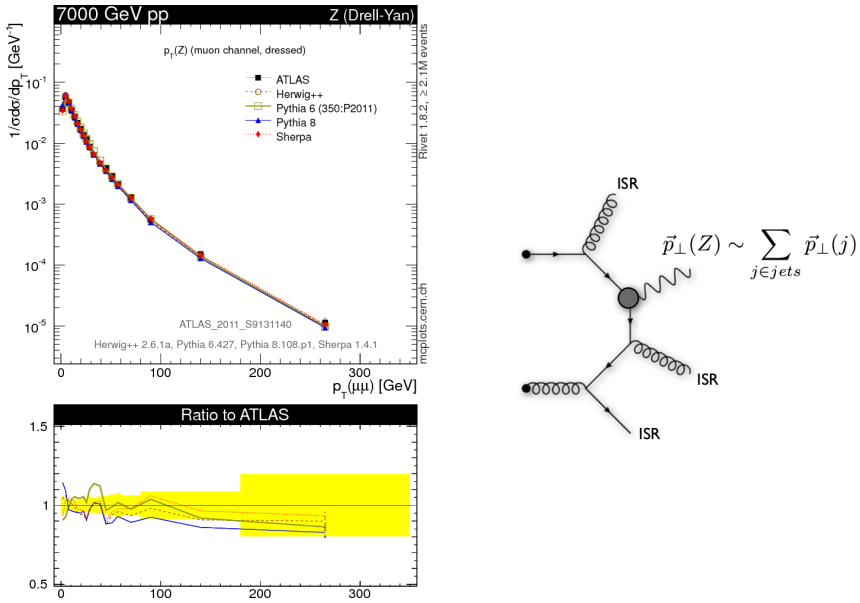

Fig. 2. The $Z/\gamma*$ transverse momentum reconstructed from the muons momenta measured by ATLAS [36].

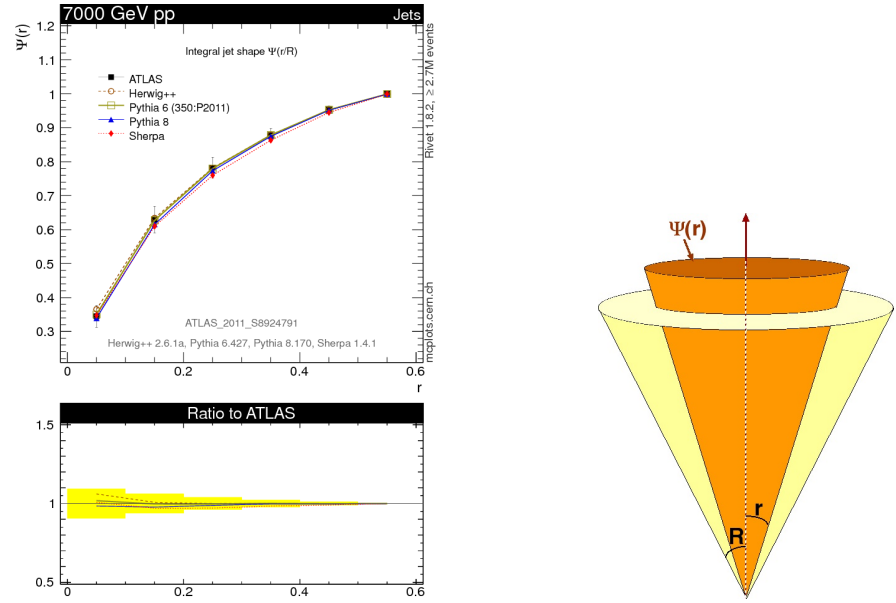

Fig. 3. The integral jet shape $\Psi(r)$ measured by ATLAS [37]. The predictions of HERWIG++, PYTHIA6, PYTHIA8 and SHERPA are shown for comparison.

within a single jet of given radius R measured by ATLAS [37] and presented in Fig. 3. $\Psi(r)$ is defined as the average fraction of the jet p_{T} that lies inside a cone of radius r concentric with the jet cone (see the left-hand side of Fig. 3). This observable show mainly sensitivity to the details of the parton shower but it is also sensitive to fragmentation, and underlying event models used in the Monte Carlo generators. Without a reasonable modelling of the latter two, the description would never be as accurate as shown in the figure.

The next useful observable directly sensitive to the QCD radiation is the di-jet azimuthal decorrelation [38] shown in Fig. 4. At the Born level, dijets are produced with equal transverse momenta p_{T} with respect to the beam axis and back-to-back in the azimuthal angle ($\Delta\phi = \pi$). Soft-gluon emission will decorrelate the two highest (leading) jets and cause small deviations from π. Larger decorrelations from π occur in the case of hard multijet production. Three-jet topologies dominate the region of $2/3\pi < \Delta\phi_{\mathrm{dijet}} < \pi$, whereas angles smaller than $2/3\pi$ are populated by four-jet events. Therefore, this observable is sensitive not only to PS evolution but also to merging of leading-order matrix elements for multijet production with parton showers (*e.g.* CKKW). Finally, the dijet azimuthal decorrelation with $\Delta\phi > 2/3\pi$ is caused, in part, by multiparton interactions which we will discuss in Section 6.

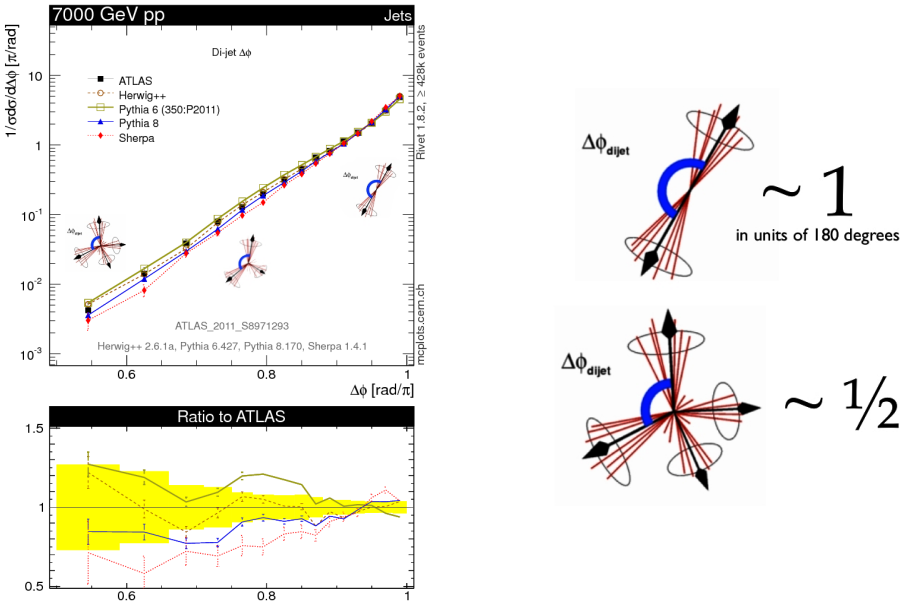

Fig. 4. ATLAS measurement of the differential cross section $(1/\sigma)(d\sigma/d\Delta\phi)$ of the azimuthal decorrelation [38]. We show results for the highest jet transverse momenta between $210 < p_{\mathrm{T}} < 260$ GeV.

5. Hadronization

There are two main models of hadronization in use, the Lund string model [39] and the Cluster model [40]. Hadronization in PYTHIA uses the Lund string fragmentation framework which is based on the observation, from lattice simulations of QCD, that at large distances the potential energy of colour sources, such as a heavy quark–antiquark pair, increases linearly with their separation, corresponding to a distance-independent force of attraction. This is thought to be due to the self-attraction of the gluonic field, causing it to collapse into a string or tube configuration with thickness of the order of 1 fm, when the separation of the sources becomes much larger than this. Hadronization in HERWIG is based on the pre-confinement property of perturbative QCD [41]. According to that, a parton shower evolving to the cut-off scale Q_0 ends up in a state of colourless parton combinations with finite mass of $\mathcal{O}(Q_0)$. In the cluster hadronization model, these parton combinations — the clusters — are interpreted as highly excited pre-hadronic states. They act as a starting point for the generation of hadrons via cluster decays, which can be performed in multiple steps. SHERPA has implemented a cluster hadronization model [42] that is quite similar to the cluster hadronization in HERWIG but differs in some details. The hadronization models have not changed much in the physical details with respect to the old fortran version of the PYTHIA and HERWIG generators. The biggest recent change in the HERWIG++ hadronization model was an introduction of the so-called colour reconnection model, which can be regarded as an extension of the cluster model but is related to multiple parton interactions, therefore, will be described in the next section.

Last but not least, the treatment of the hadronic decays plays an important role in the simulation because in both the string and the cluster models it is rare that the clusters decay directly to the stable hadrons like pions and kaons which are observed in the detector. Most of the time, they decay to higher resonances, which then decay further to stable particles. The current decays models are very sophisticated, including matrix elements for many modes and spin correlations. They also take into account effects such as photon radiation in the decay of hadrons [43, 44].

6. Multiple parton interactions

In a hadron–hadron collision more than one pair of partons may interact, leading to the possibility of multiple interactions (additional semi-hard partonic scatters). These additional semi-hard scatters should be dressed with the additional radiations via parton shower evolution and must be properly connected to the hadronization models. The first detailed Monte Carlo model for the perturbative MPI was proposed in [45] and was the main

model in PYTHIA for a long time. The models implemented in HERWIG++ and SHERPA are based on similar physical picture. There are, however, important details where the approach deviates from the formalism in PYTHIA, for details see [2]. For example, in the recent PYTHIA versions, the additional hard scatters are interleaved with the parton shower [26, 27] which is not the case in SHERPA or HERWIG++. This approach allows a picture where MPI and the parton shower radiation are interleaved in one common sequence of decreasing $p_\perp$ values. There is also a new approach to MPI in SHERPA called SHRiMPS. It aims at a smooth inclusion of diffractive and soft interactions into the multiple iteraction picture, based on a Gribov–Regge formalism [46]. In Fortan HERWIG, the UE had been modelled in an additional package JIMMY [47] that has added additional hard scatters to the HERWIG simulation. The model had also been extended to include an additional soft component [48]. Similar models with hard and soft component of multiple partonic interactions are also available in HERWIG++ [49, 50]. In HERWIG++, there were also details studies on the colour structure of multiple interactions leading to construction of abovementioned colour reconnection (CR) model [51]. The idea of CR is based on colour preconfinement [41], which implies that parton jets emerging from different partonic interactions are colour-connected (clustered) if they are located closely in phase space. As the MPI model does not take that into account, those colour connections have to be adapted afterwards by means of a CR procedure. The CR model define the distance between two partons based on their invariant mass, *i.e.* the distance is small when their invariant mass (cluster mass) is small. Therefore, the aim of the CR model is to reduce the colour length $\lambda \equiv \sum_{i=1}^{N_{\mathrm{cl}}} m_i^2$, where N_{cl} is the number of clusters in an event and m_i is the invariant mass of cluster i. A similar model of CR was implemented some time ago in PYTHIA [6]. To visualize that the colour structure of the event can cause non-trivial changes to the colliding system as a whole, with potentially major consequences for the particle multiplicity in the final state we show Fig. 5, which presents the Minimum Bias data from ATLAS [52, 53]. We can clearly see that the MPI model without improved treatment of CR in HERWIG++ was too simple to describe the data. The next important test of the MPI models is whether they are able to describe the UE data collected at different collider energies [54, 55]. The standard UE measurements are made relative to a leading object (the hardest charged track or jet). Then, the transverse plane is subdivided in azimuthal angle ϕ relative to this leading object at $\phi = 0$. The region around the leading object, $|\phi| < \pi/3$, is called the "towards" region. The opposite region, where we usually find a recoiling hard leading object, $|\phi| > 2\pi/3$, is called "away" region, while the remaining region, transverse to the leading object and its recoil, where the underlying event is expected to be least "contaminated" by

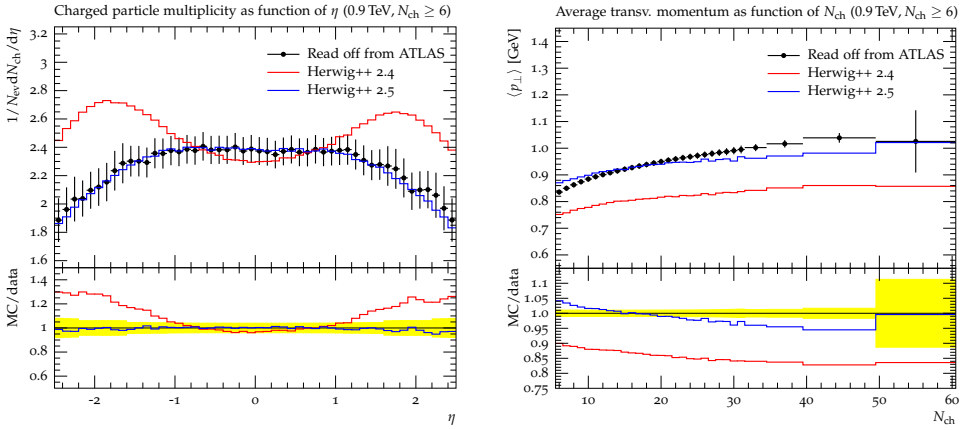

Fig. 5. Comparison of HERWIG 2.4.2 without CR and HERWIG 2.5 with CR to ATLAS minimum-bias distributions at $\sqrt{s} = 0.9$ TeV.

activity from the hard subprocess, is called "transverse" region. Therefore, in Figs. 6 and 7 we show the mean number of stable charged particles per unit of η–ϕ, $d^2N_{\mathrm{ch}}/d\eta d\phi$, and the mean scalar $p_\perp$ sum of stable particles both as a function of $p_\perp^{\mathrm{lead}}$ in the transverse region. Figures 6 and 7 show nicely that the transverse activity decouples from the leading object momentum for large momenta, as a plateau is formed, hence the correct interpretation as underlying event activity. We can also see that all MCEG describe the

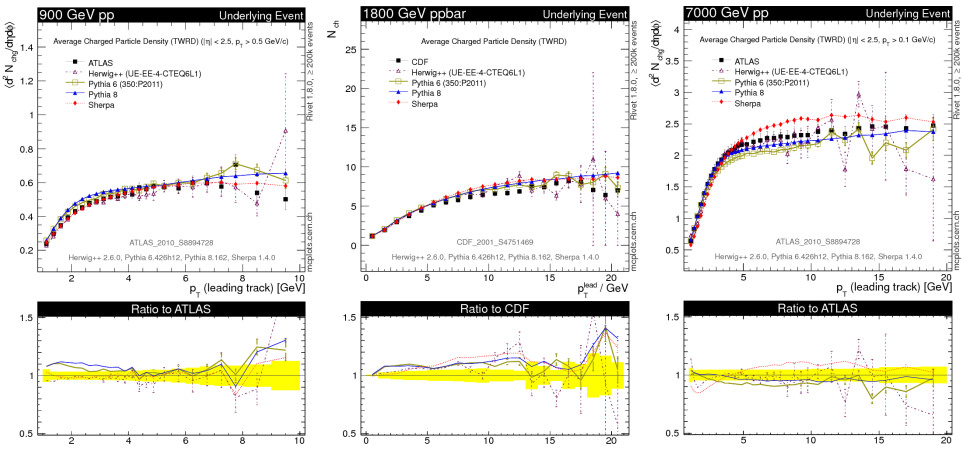

Fig. 6. ATLAS data at 900 GeV (1st column), CDF data at 1800 GeV (2nd column) and ATLAS data at 7 TeV (3rd column), showing the multiplicity density of the charged particles in the "transverse" area as a function of $p_\perp^{\mathrm{lead}}$.

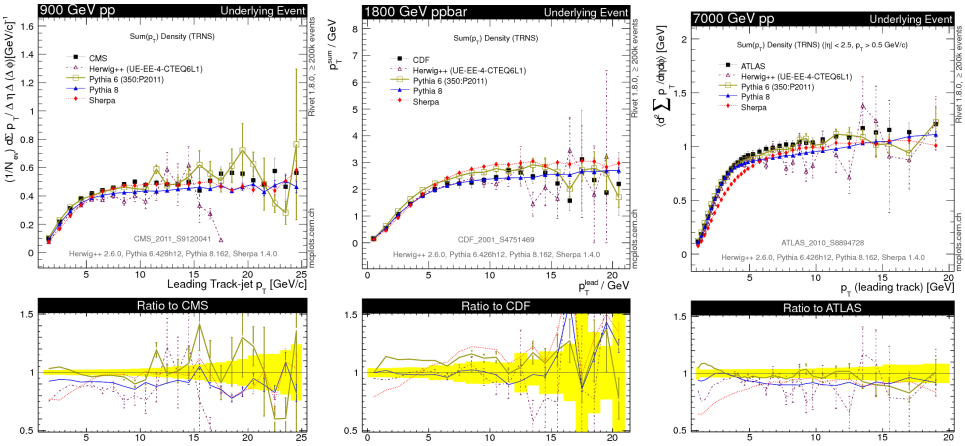

Fig. 7. ATLAS data at 900 GeV (1st column), CDF data at 1800 GeV (2nd column) and ATLAS data at 7 TeV (3rd column), showing the mean scalar $p_\perp$ sum of the stable charged particles in the "transverse" area as a function of $p_\perp^{\text{lead}}$.

data collected at different collider energies reasonably well, which would not be possible without good modelling of MPI. In the left-hand side panel of Fig. 8, we see that UE tunes (except SHERPA which does not have a CR model) are able to describe $\langle p_{\text{t}} \rangle$ *versus* N_{ch} MB data collected at 7 TeV when charged particles are not too soft with $p_\perp > 500$ MeV. On the other hand, as can be seen on the right hand-side plot in Fig. 8, all UE tunes fail to reproduce the ATLAS MB data when softer charged particles with $p_\perp > 100$ MeV are taken into account. The unsatisfactory description of the $\langle p_{\text{t}} \rangle$ *versus* N_{ch} observable in the high multiplicity tail may indicate missing physics in the MCEG models. It is worth to mention that the cosmic-rays model EPOS [56, 57] seems to be able to describe MB data well but on the other hand it fails with the description of the UE data.

The other important problem of the MPI models which needs to be solved, is a disagreement with the CDF's measurement of the double parton scattering cross section [58]. In the recent publication [59], the authors reanalyzed CDF's event definition to provide an improved value of

$$\sigma_{\text{eff}} = \left(12.0 \pm 1.4^{+1.3}_{-1.5}\right) \text{ mb}\,, \tag{1}$$

which is the normalization factor that relates the cross section for double parton scattering to the product of the inclusive cross sections of the two individual scatters. The obtained value of σ_{eff} should serves as a constraint on the Monte Carlo models since the recent tunes of the MPI models to the LHC data predict its value to be between 25–42 mb [60].

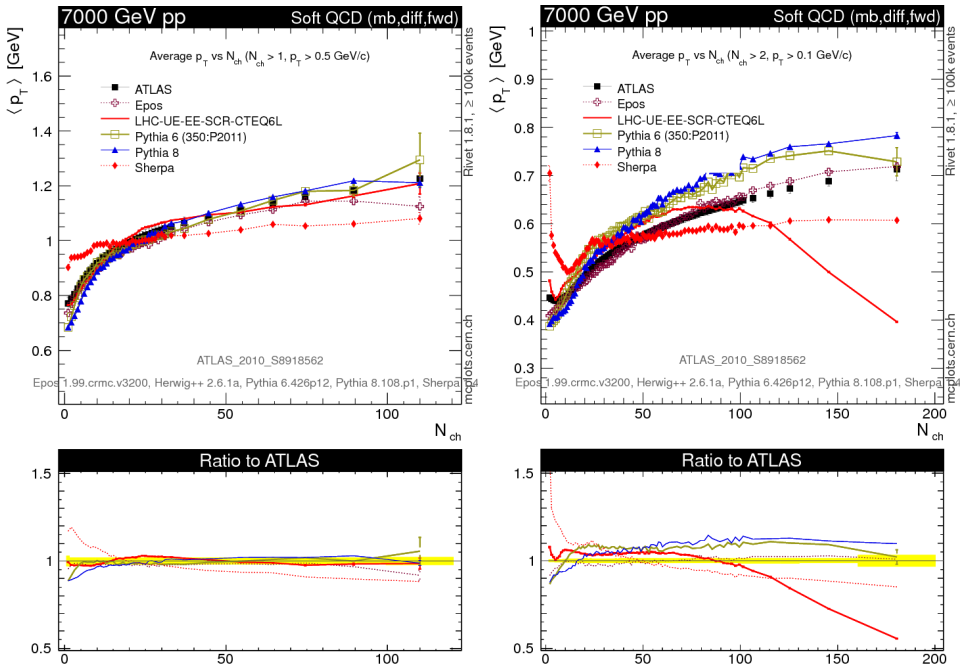

Fig. 8. ATLAS data showing the average transverse momentum as a function of the number of charged particles in the event for events with the $p_\perp > 500$ MeV (left panel) and $p_\perp > 100$ MeV (right panel). The dots represent the data and the curves the predictions from different MC models.

7. Summary

Tremendous progress has been made in the development of MCEG over the last 30 years. To illustrate how much progress has been done just in the last five years, let us show the outlook from a talk given here, in Kraków, at the Epiphany Conference in 2007 by Gieseke [61], see Fig. 9.

We can see that all plans stated in the "Future of HERWIG++" from the talk came true. The progression of the MCEG let the modern versions of the programs to become crucial tools for LHC studies. We have seen that a wide range of LHC data is well described by MCEG, proving that all the building blocks of the programs are well established. The other LHC data sets led to new developments of the MC event generators, for example of the HERWIG++ MPI model to include non-perturbative colour reconnections. Finally, there are data sets which shows that there is still need for further developments. Since the LHC studies more rare phenomena and more subtle effects, generators must keep up by increased precision. This is only possible

with continuous dialogue with experimental community, can be enhanced by more powerful computational techniques and computers and must be based on new ideas.

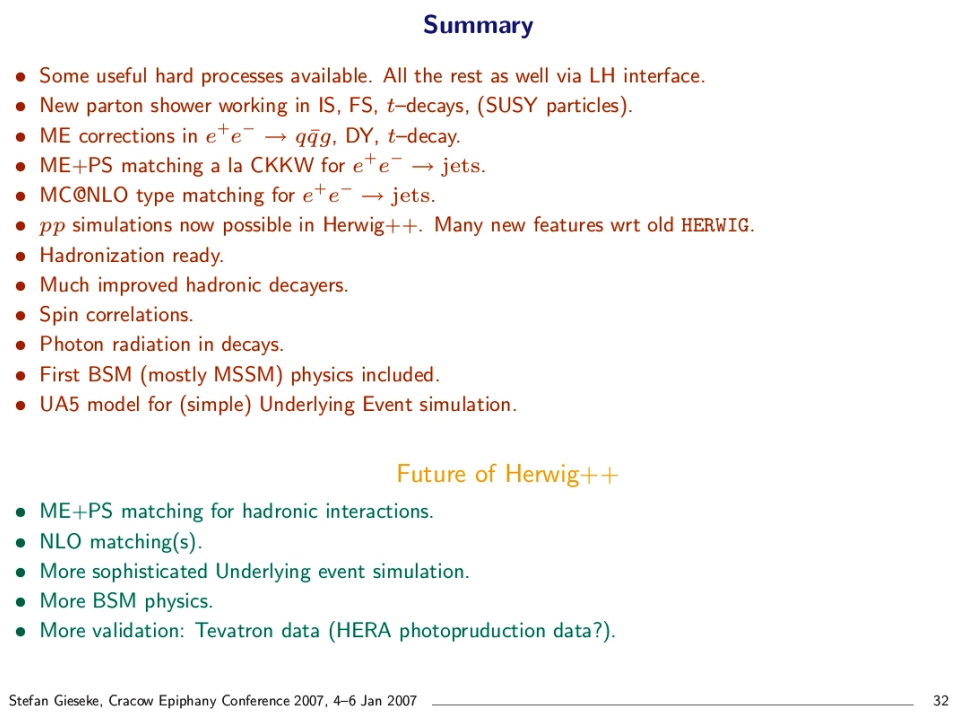

Fig. 9. The last slide from the talk "LHC Event Generation with HERWIG++" presented by Stefan Gieseke at the Cracow Epiphany Conference 2007.

We thank the Organizers for the very pleasant and fruitful workshop. This work has been supported by the Lancaster–Manchester–Sheffield Consortium for Fundamental Physics under STFC grant ST/J000418/1 and by the MCnetITN FP7 Marie Curie Initial Training Network PITN-GA-2012-315877. We wish to acknowledge Sebastian Sapeta for his critical reading of this proceedings.

REFERENCES

[1] Talk given by J.D. Bjorken at the 75th anniversary celebration of the Max-Planck Institute of Physics, Munich, Germany, December 10th, 1992. As quoted in: Beam Line, Winter 1992, Vol. 22, No. 4.

[2] A. Buckley *et al.*, *Phys. Rep.* **504**, 145 (2011) [arXiv:1101.2599 [hep-ph]].

[3] M. Bahr *et al.*, *Eur. Phys. J.* **C58**, 639 (2008) [arXiv:0803.0883 [hep-ph]].

[4] S. Gieseke *et al.*, arXiv:1102.1672 [hep-ph].

[5] K. Arnold *et al.*, arXiv:1205.4902 [hep-ph].

[6] T. Sjostrand, S. Mrenna, P.Z. Skands, *J. High Energy Phys.* **0605**, 026 (2006) [arXiv:hep-ph/0603175].

[7] T. Sjostrand, S. Mrenna, P.Z. Skands, *Comput. Phys. Commun.* **178**, 852 (2008) [arXiv:0710.3820 [hep-ph]].

[8] T. Gleisberg *et al.*, *J. High Energy Phys.* **0402**, 056 (2004) [arXiv:hep-ph/0311263].

[9] T. Gleisberg *et al.*, *J. High Energy Phys.* **0902**, 007 (2009) [arXiv:0811.4622 [hep-ph]].

[10] S. Gieseke, *Nucl. Phys. Proc. Suppl.* **222-224**, 174 (2012).

[11] T. Sjostrand, B. Soderberg, "A Monte Carlo Program For Quark Jet Generation", LU TP 78-18.

[12] S. Catani, F. Krauss, R. Kuhn, B.R. Webber, *J. High Energy Phys.* **0111**, 063 (2001) [arXiv:hep-ph/0109231].

[13] T. Gleisberg, S. Hoeche, *J. High Energy Phys.* **0812**, 039 (2008) [arXiv:0808.3674 [hep-ph]].

[14] F. Krauss, R. Kuhn, G. Soff, *J. High Energy Phys.* **0202**, 044 (2002) [arXiv:hep-ph/0109036].

[15] M.A. Gigg, P. Richardson, *Eur. Phys. J.* **C51**, 989 (2007) [arXiv:hep-ph/0703199].

[16] M.A. Gigg, P. Richardson, arXiv:0805.3037 [hep-ph].

[17] N. Desai, P.Z. Skands, *Eur. Phys. J.* **C72**, 2238 (2012) [arXiv:1109.5852 [hep-ph]].

[18] M.J. Dolan *et al.*, *J. High Energy Phys.* **1106**, 095 (2011) [arXiv:1104.0585 [hep-ph]].

[19] J. Alwall *et al.*, *J. High Energy Phys.* **1106**, 128 (2011) [arXiv:1106.0522 [hep-ph]].

[20] J. Alwall *et al.*, *Comput. Phys. Commun.* **176**, 300 (2007) [arXiv:hep-ph/0609017].

[21] A. van Hameren, *Acta Phys. Pol. B* **44**, 1629 (2013), this issue.

[22] G. Corcella *et al.*, *J. High Energy Phys.* **0101**, 010 (2001) [arXiv:hep-ph/0011363].

[23] G. Corcella *et al.*, arXiv:hep-ph/0210213.

[24] S. Gieseke, P. Stephens, B. Webber, *J. High Energy Phys.* **0312**, 045 (2003) [arXiv:hep-ph/0310083].

[25] S. Gieseke, M.H. Seymour, A. Siodmok, *J. High Energy Phys.* **0806**, 001 (2008) [arXiv:0712.1199 [hep-ph]].

[26] T. Sjostrand, P.Z. Skands, *J. High Energy Phys.* **0403**, 053 (2004) [arXiv:hep-ph/0402078].

[27] T. Sjostrand, P.Z. Skands, *Eur. Phys. J.* **C39**, 129 (2005) [arXiv:hep-ph/0408302].

[28] S. Schumann, F. Krauss, *J. High Energy Phys.* **0803**, 038 (2008) [arXiv:0709.1027 [hep-ph]].

[29] S. Catani, M.H. Seymour, *Nucl. Phys.* **B485**, 291 (1997) [*Erratum ibid. Nucl. Phys.* **B510**, 503 (1998)] [arXiv:hep-ph/9605323].

[30] J.C. Winter, F. Krauss, *J. High Energy Phys.* **0807**, 040 (2008) [arXiv:0712.3913 [hep-ph]].

[31] L. Lonnblad, *Comput. Phys. Commun.* **71**, 15 (1992).

[32] S. Platzer, S. Gieseke, *Eur. Phys. J.* **C72**, 2187 (2012) [arXiv:1109.6256 [hep-ph]].

[33] W.T. Giele, D.A. Kosower, P.Z. Skands, *Phys. Rev.* **D78**, 014026 (2008).

[34] W.T. Giele, D.A. Kosower, P.Z. Skands, *Phys. Rev.* **D84**, 054003 (2011) [arXiv:1102.2126 [hep-ph]].

[35] A. Gehrmann-De Ridder, M. Ritzmann, P. Skands, *Phys. Rev.* **D85**, 014013 (2012) [arXiv:1108.6172 [hep-ph]].

[36] G. Aad *et al.* [ATLAS Collaboration], *Phys. Lett.* **B705**, 415 (2011) [arXiv:1107.2381 [hep-ex]].

[37] G. Aad *et al.* [Atlas Collaboration], *Phys. Rev.* **D83**, 052003 (2011) [arXiv:1101.0070 [hep-ex]].

[38] G. Aad *et al.* [ATLAS Collaboration], *Phys. Rev. Lett.* **106**, 172002 (2011) [arXiv:1102.2696 [hep-ex]].

[39] B. Andersson, G. Gustafson, G. Ingelman, T. Sjostrand, *Phys. Rep.* **97**, 31 (1983).

[40] B.R. Webber, *Nucl. Phys.* **B238**, 492 (1984).

[41] D. Amati, G. Veneziano, *Phys. Lett.* **B83**, 87 (1979).

[42] J.C. Winter, F. Krauss, G. Soff, *Eur. Phys. J.* **C36**, 381 (2004) [arXiv:hep-ph/0311085].

[43] K. Hamilton, P. Richardson, *J. High Energy Phys.* **0607**, 010 (2006) [arXiv:hep-ph/0603034].

[44] M. Schonherr, F. Krauss, *J. High Energy Phys.* **0812**, 018 (2008) [arXiv:0810.5071 [hep-ph]].

[45] T. Sjostrand, M. van Zijl, *Phys. Rev.* **D36**, 2019 (1987).

[46] V.A. Khoze *et al.*, *Eur. Phys. J.* **C69**, 85 (2010) [arXiv:1005.4839 [hep-ph]].

[47] J.M. Butterworth, J.R. Forshaw, M.H. Seymour, *Z. Phys.* **C72**, 637 (1996) [arXiv:hep-ph/9601371].

[48] I. Borozan, M.H. Seymour, *J. High Energy Phys.* **0209**, 015 (2002) [arXiv:hep-ph/0207283].

[49] M. Bahr, S. Gieseke, M.H. Seymour, *J. High Energy Phys.* **0807**, 076 (2008) [arXiv:0803.3633 [hep-ph]].

[50] M. Bahr, J.M. Butterworth, S. Gieseke, M.H. Seymour, arXiv:0905.4671 [hep-ph].

[51] S. Gieseke, C. Rohr, A. Siodmok, *Eur. Phys. J.* **C72**, 2225 (2012) [arXiv:1206.0041 [hep-ph]].

[52] G. Aad *et al.* [ATLAS Collaboration], *Phys. Lett.* **B688**, 21 (2010).

[53] G. Aad *et al.* [ATLAS Collaboration], *New J. Phys.* **13**, 053033 (2011).

[54] T. Affolder *et al.* [CDF Collaboration], *Phys. Rev.* **D65**, 092002 (2002).

[55] G. Aad *et al.* [Atlas Collaboration], *Phys. Rev.* **D83**, 112001 (2011).

[56] H.J. Drescher *et al.*, *Phys. Rep.* **350**, 93 (2001) [arXiv:hep-ph/0007198].

[57] K. Werner *et al.*, *Phys. Rev.* **C82**, 044904 (2010) [arXiv:1004.0805 [nucl-th]].

[58] F. Abe *et al.* [CDF Collaboration], *Phys. Rev.* **D56**, 3811 (1997).

[59] M. Bahr, M. Myska, M.H. Seymour, A. Siodmok, *J. High Energy Phys.* **1303**, 129 (2013) [arXiv:1302.4325 [hep-ph]].

[60] S. Gieseke, C.A. Röhr, A. Siódmok, arXiv:1110.2675 [hep-ph].

[61] S. Gieseke, *Acta Phys. Pol. B* **38**, 2261 (2007).